Electronic Supplementary Information

Enhanced Stability of Boron Modified NiFe Hydroxide for Oxygen Evolution Reaction

Yewon Hong [a,‡], *Juhyung Choi* [a,‡], *Eunchong Lee* [a], *Yun Jeong Hwang* [a, b*]

[a] Department of Chemistry, College of Natural Sciences, Seoul National University (SNU), Seoul 08826, Republic of Korea

[b] Center for Nanoparticle Research, Institute for Basic Science (IBS), Seoul 08826, Republic of Korea

‡ These authors equally contributed to this work.

Corresponding author: yjhwang1@snu.ac.kr

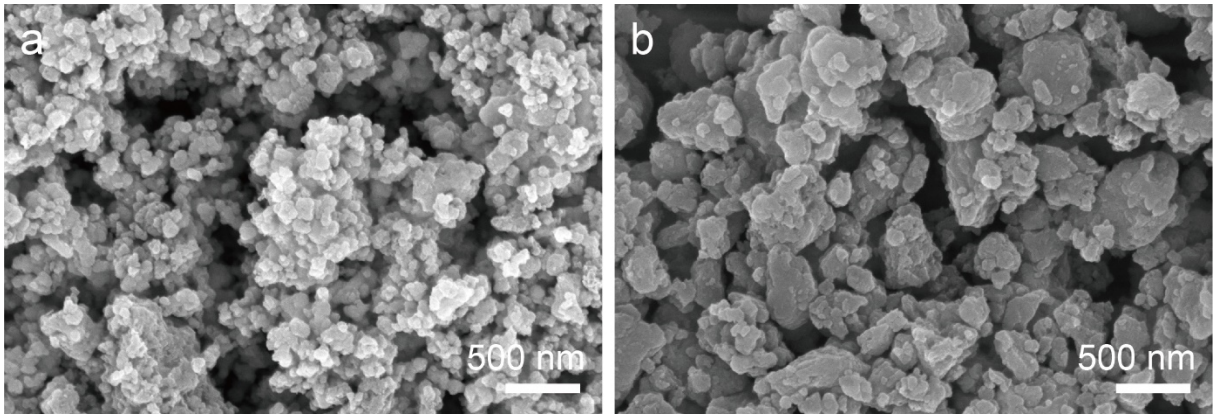

Fig. S1. SEM images of (a) B-$NiFeO_xH_y$ and (b) $NiFeO_xH_y$.

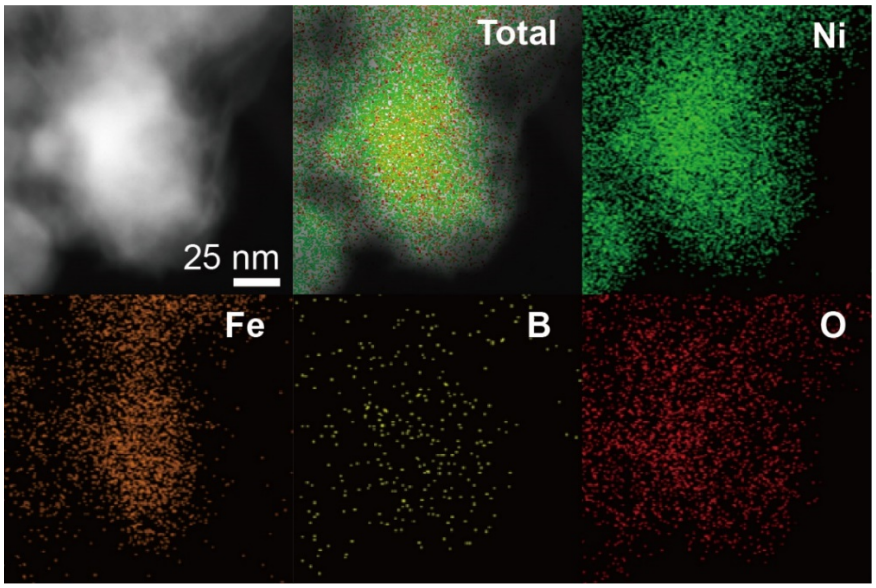

Fig. S2. EDX mapping images of sr_B-$NiFeO_xH_y$, tilted at 15 degrees. Note that due to the small scattering angle of the boron, the sample was tilted at 15 degrees to obtain the signal of the B from the B-$NiFeO_xH_y$ catalyst.

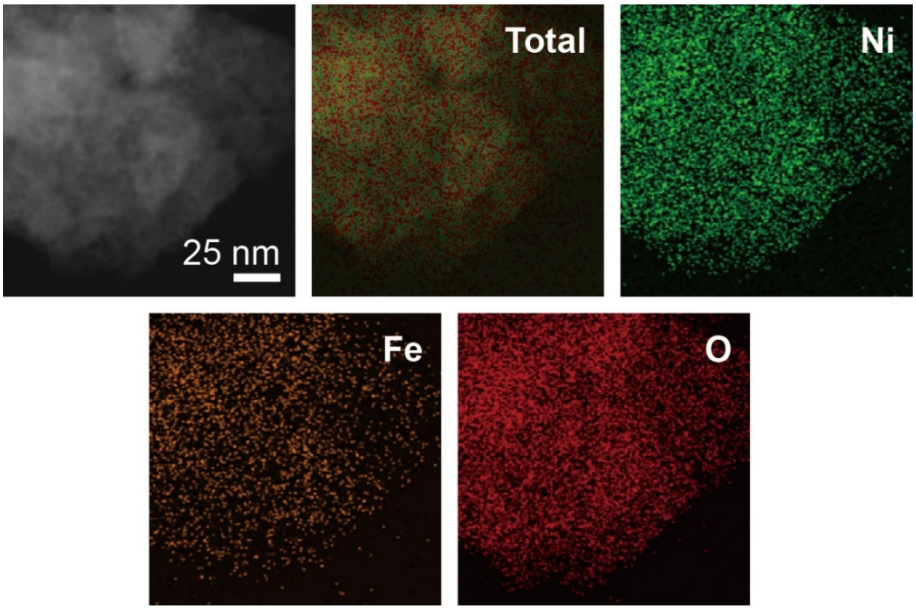

Fig. S3. EDX mapping images of $NiFeO_xH_y$, untilted.

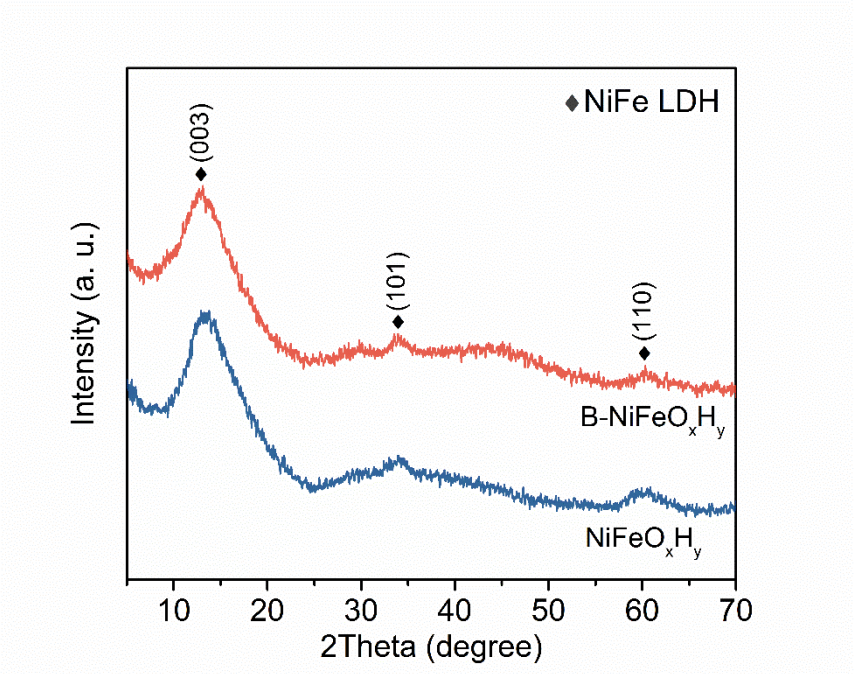

Fig. S4. XRD patterns of B-$NiFeO_xH_y$ and $NiFeO_xH_y$.

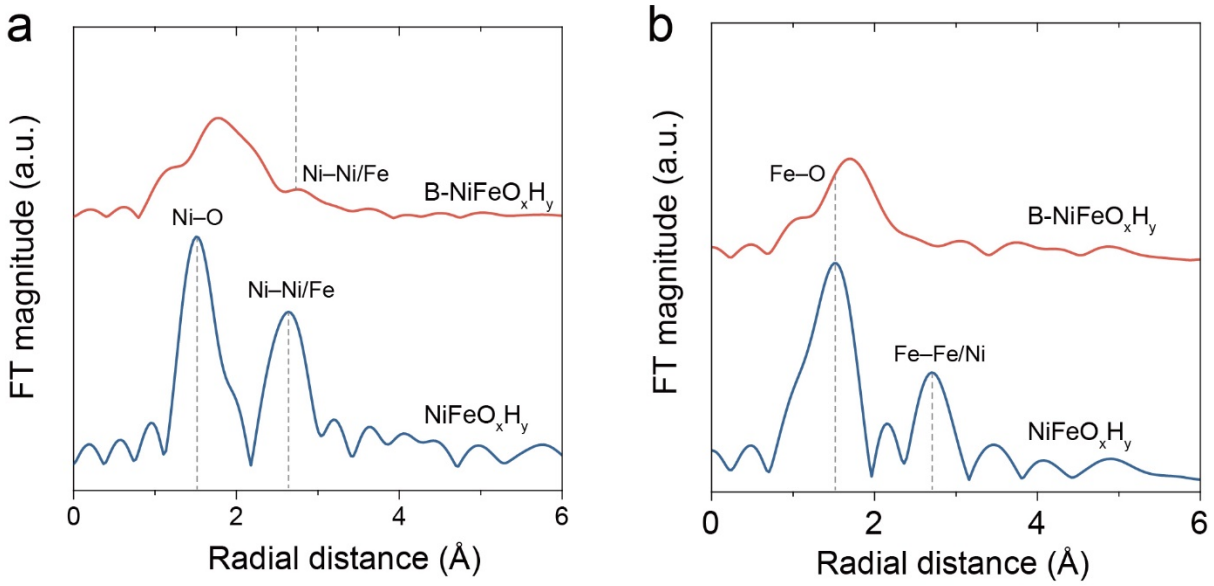

Fig. S5. The normalized (a) Ni and (b) Fe K-edge EXAFS analyses of B-NiFeO$_x$H$_y$ and NiFeO$_x$H$_y$.

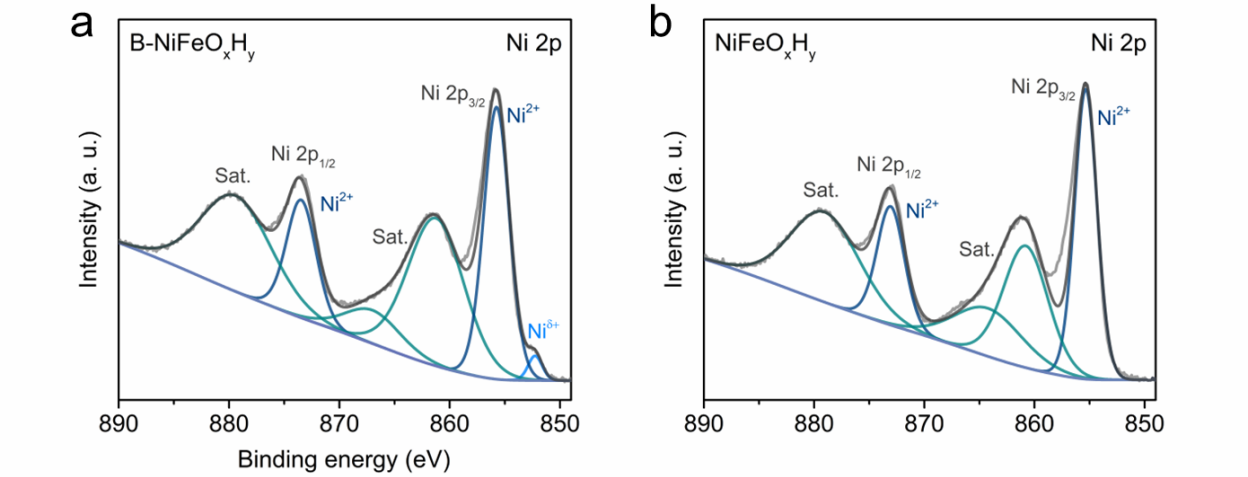

Fig. S6. High-resolution XPS spectra of (a) B-NiFeO$_x$H$_y$ and (b) NiFeO$_x$H$_y$ in Ni 2p.

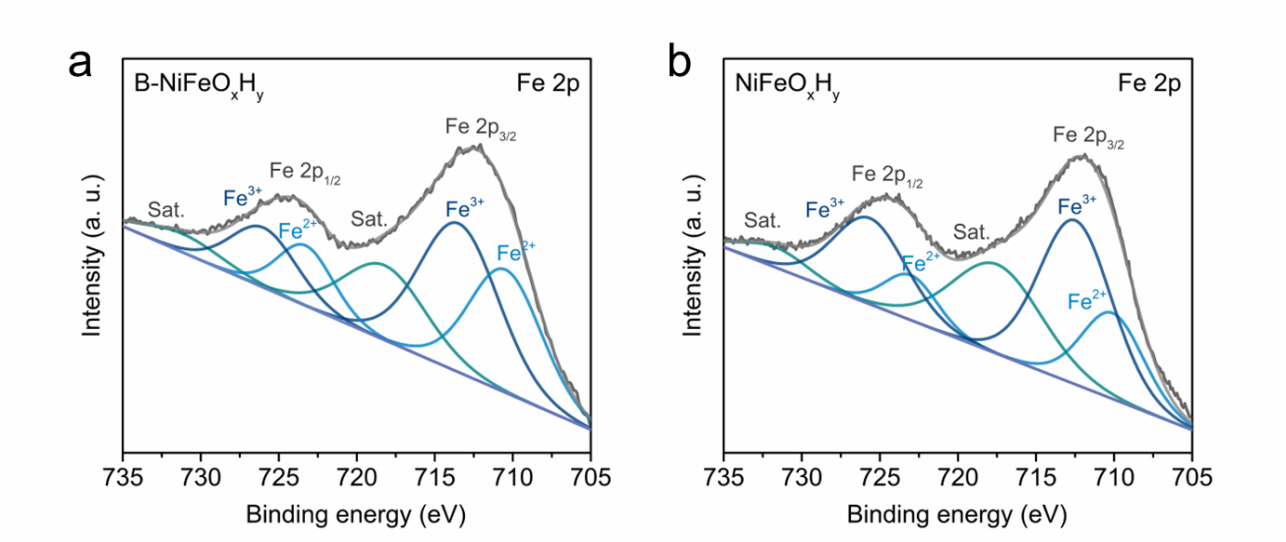

Fig. S7. High-resolution XPS spectra of (a) B-NiFeO$_x$H$_y$ and (b) NiFeO$_x$H$_y$ in Fe 2p.

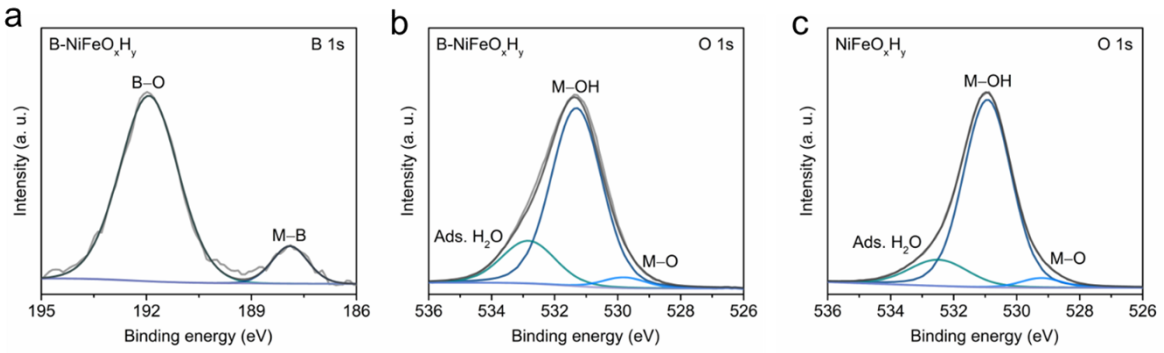

Fig. S8. High-resolution XPS B 1s spectra of (a) B-NiFeO$_x$H$_y$ and O 1s spectra of (b) B-NiFeO$_x$H$_y$ and (c) NiFeO$_x$H$_y$.

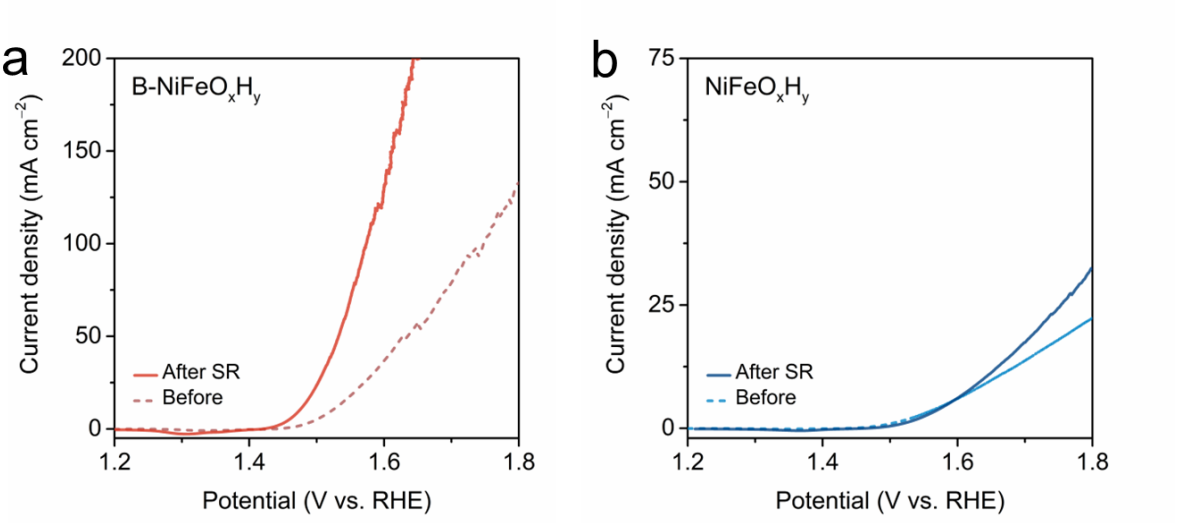

Fig. S9. LSV curves of (a) B-NiFeO$_x$H$_y$ and (b) NiFeO$_x$H$_y$ before and after electro-driven surface-reconstruction process at a scan rate of 5 mV s^{-1}.

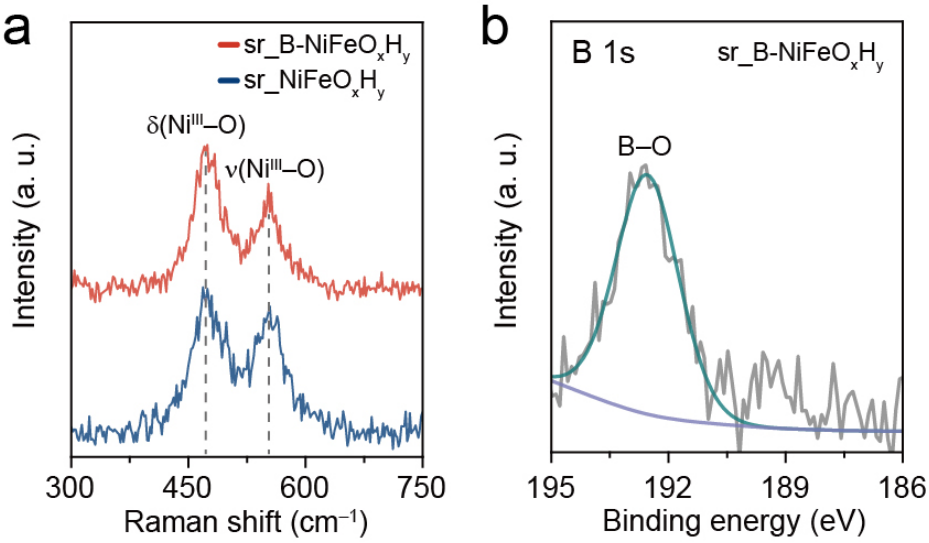

Fig. S10. (a) Raman spectra of sr_B-NiFeO$_x$H$_y$ and sr_NiFeO$_x$H$_y$ after electro-driven surface-reconstruction process. (b) High-resolution B 1s spectrum of sr_B-NiFeO$_x$H$_y$.

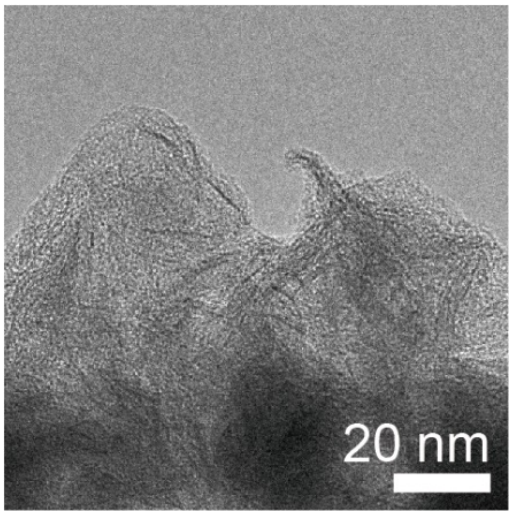

Fig. S11. TEM image of sr_B-$NiFeO_xH_y$.

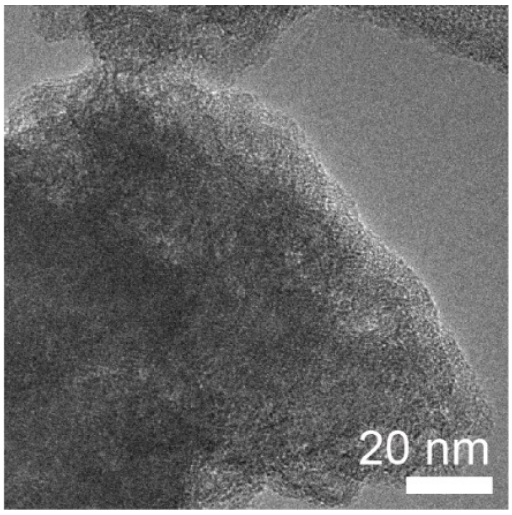

Fig. S12. TEM image of sr_$NiFeO_xH_y$.

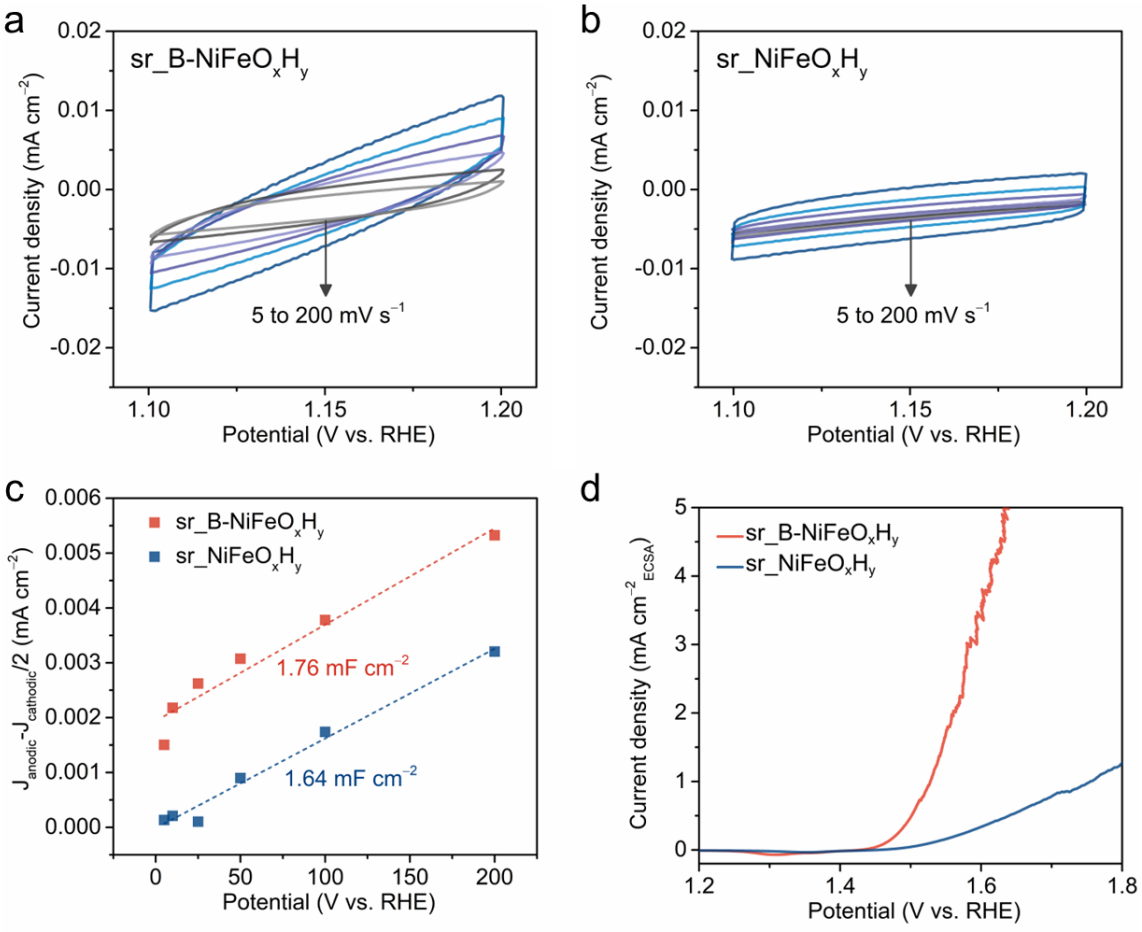

Fig. S13. Cyclic voltammograms of (a) sr_B-NiFeO$_x$H$_y$ and (b) sr_NiFeO$_x$H$_y$ in a non-Faradaic region at various scan rates from 5 to 200 mV s^{-1}. (c) Capacitive currents of the sr-catalysts plotted as a function of scan rate and (d) LSV curves of the sr-catalyts normalized by ECSA.

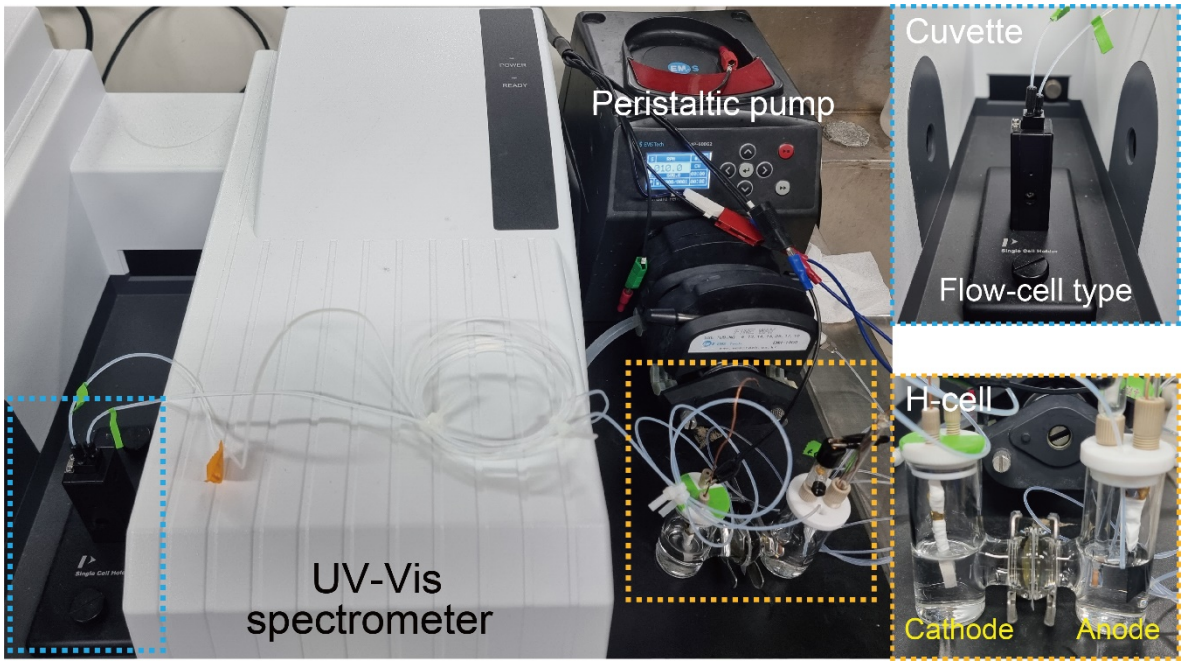

Fig. S14. Photograph of Operando UV-Vis spectroelectrochemical system.

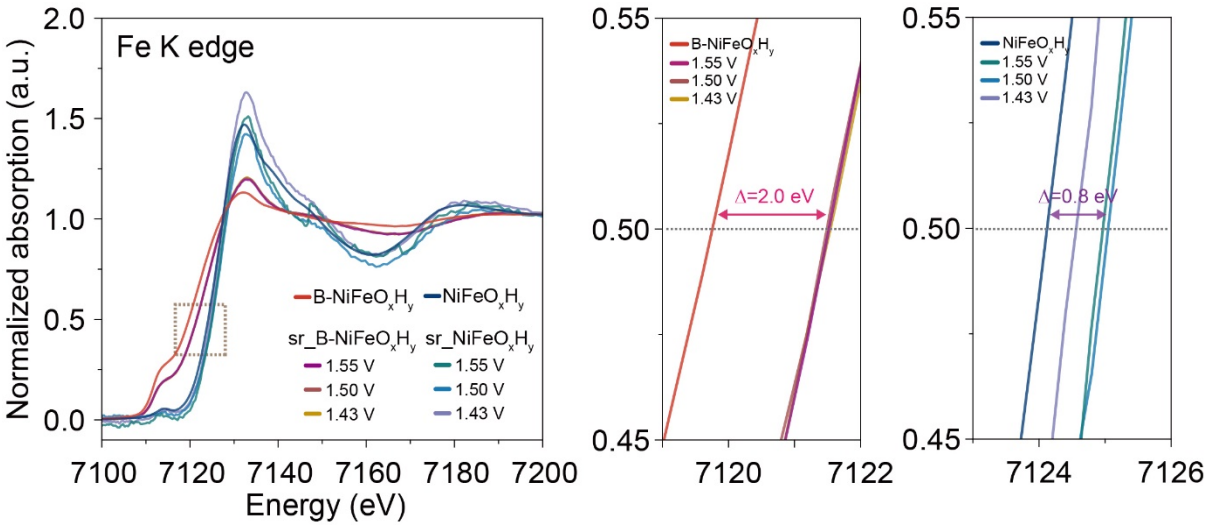

Fig. S15. Operando normalized Fe K-edge XANES analysis at various potential conditions of sr_B-$NiFeO_xH_y$ and sr_$NiFeO_xH_y$. Magnification of the corresponding regions related to the pre-edge XANES regions.

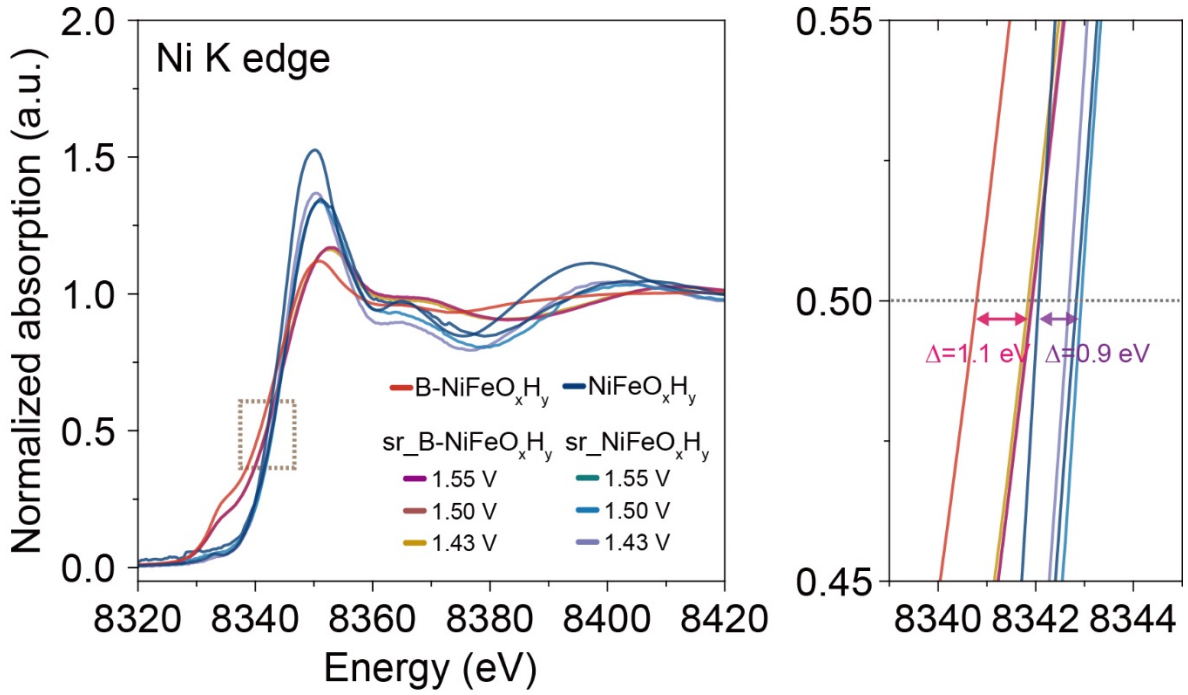

Fig. S16. Operando normalized Ni K-edge XANES analysis at various potential conditions of sr_B-NiFeO$_x$H$_y$ and sr_NiFeO$_x$H$_y$. Magnification of the corresponding regions related to the pre-edge XANES regions.

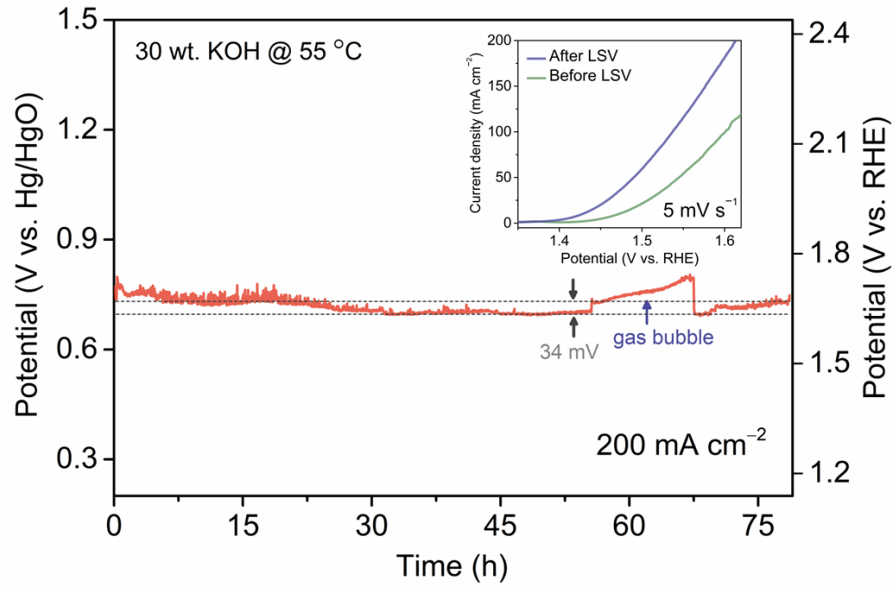

Fig. S17. Chronopotentiometric curve of sr_$NiFeO_xH_y$ at a current density of 200 mA cm^{-2} in 30 wt% KOH under 55 ºC. Inset indicates LSV curves of before and after stability test without iR compensation.

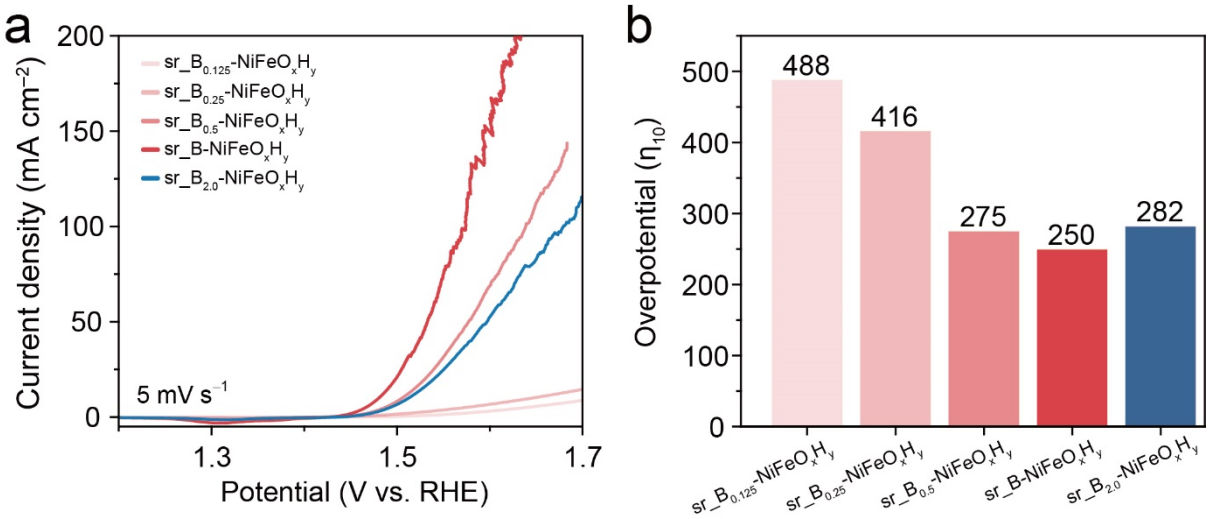

Fig. S18. (a) LSV curves and (b) overpotentials at 10 mA cm^{-2} of sr_B-NiFeO$_x$H$_y$ with varying boron amounts in 1 M KOH. The boron amounts were varied by adding 0.125, 0.25, 0.5, and 2 times of the $NaBH_4$ added during the synthesis process.

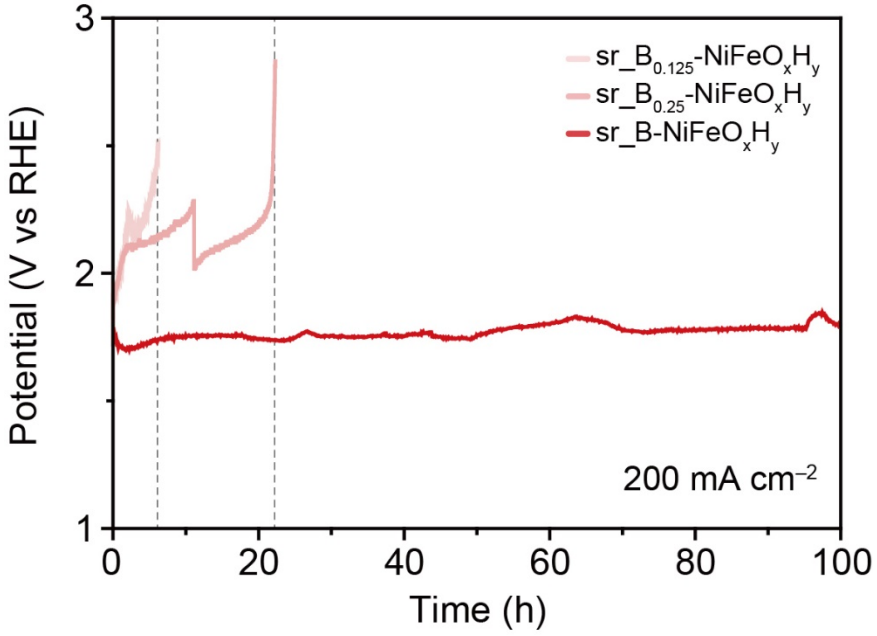

Fig. S19. Long-term stability test at 200 mA cm^{-2} in 1 M KOH of sr_B-$NiFeO_xH_y$ with varying B amounts in 1 M KOH. The dotted lines in a graph represent the durabilities of sr_$B_{0.125}$-$NiFeO_xH_y$ and sr_$B_{0.25}$-$NiFeO_xH_y$, which are 6 h and 22 h, respectively. Fluctuations during the stability tests are owing to bubble formation near the reference electrode.

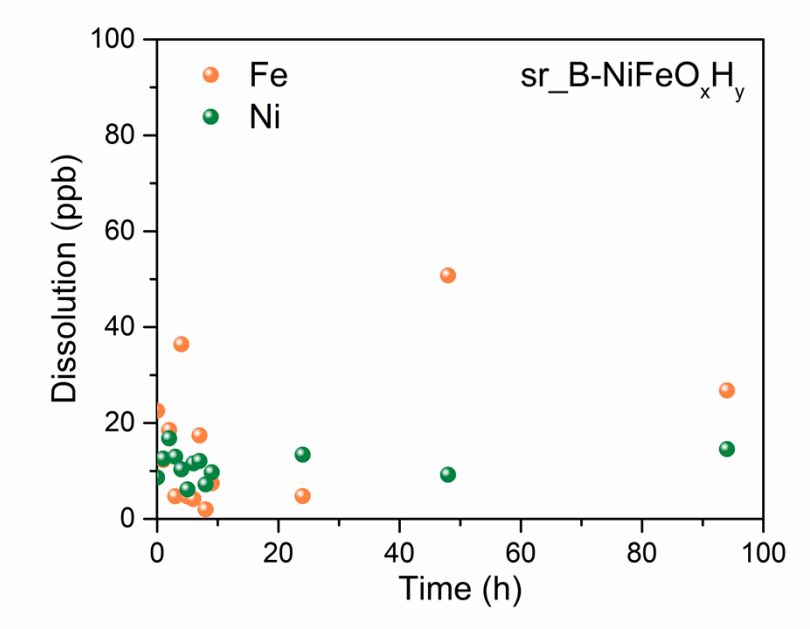

Fig. S20. ICP-MS trace of sr_B-NiFeO$_x$H$_y$ during the long-term stability test.

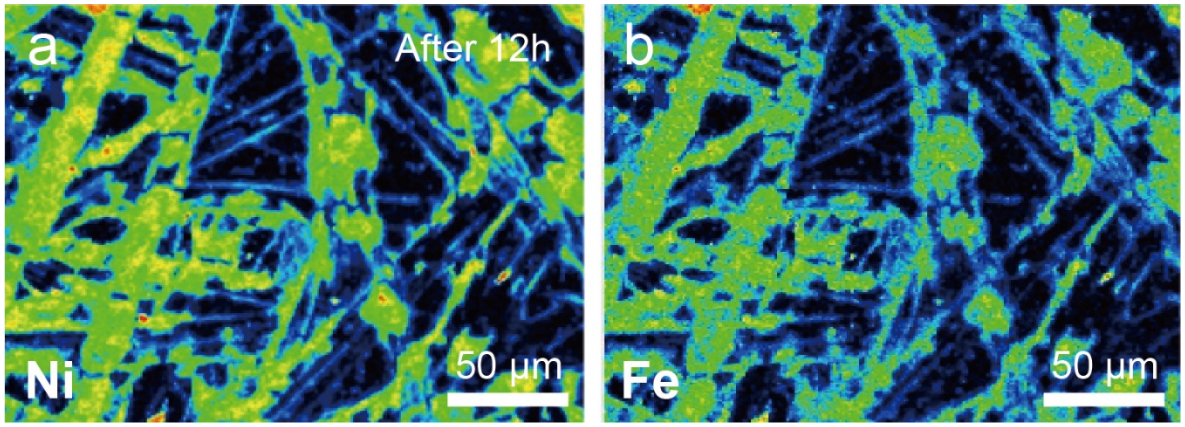

Fig. S21. EPMA of sr_B-NiFeO$_x$H$_y$ for (a) Ni and (b) Fe after 12 hours at a current density of 200 mA cm^{-2}.

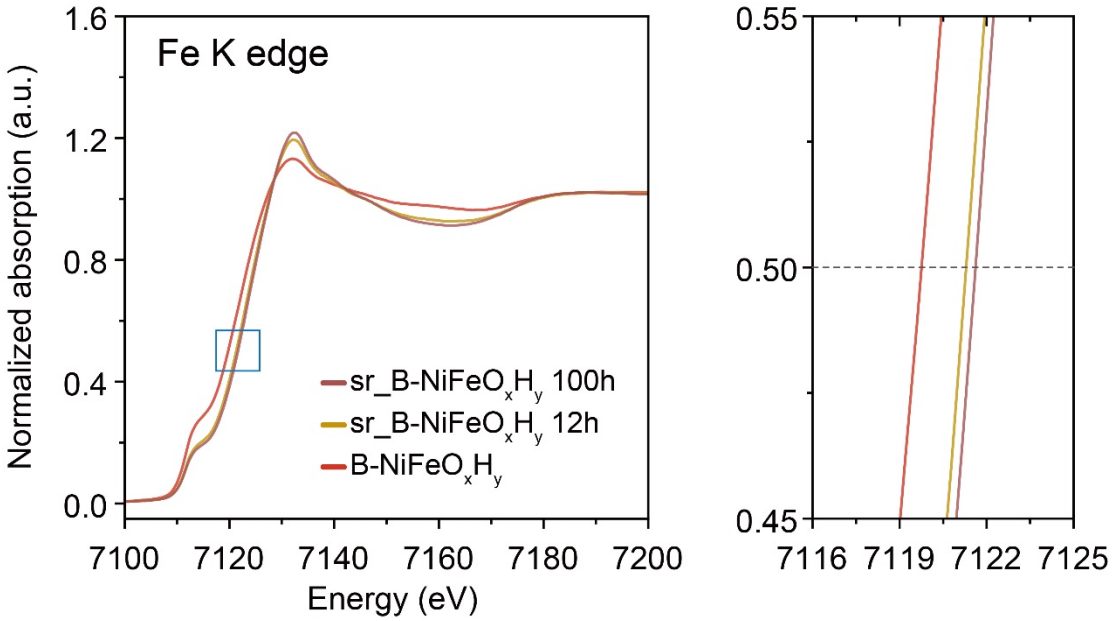

Fig. S22. The normalized Fe K-edge XAS analyses of B-NiFeO$_x$H$_y$ before and after 12 h and 100 h stability test.

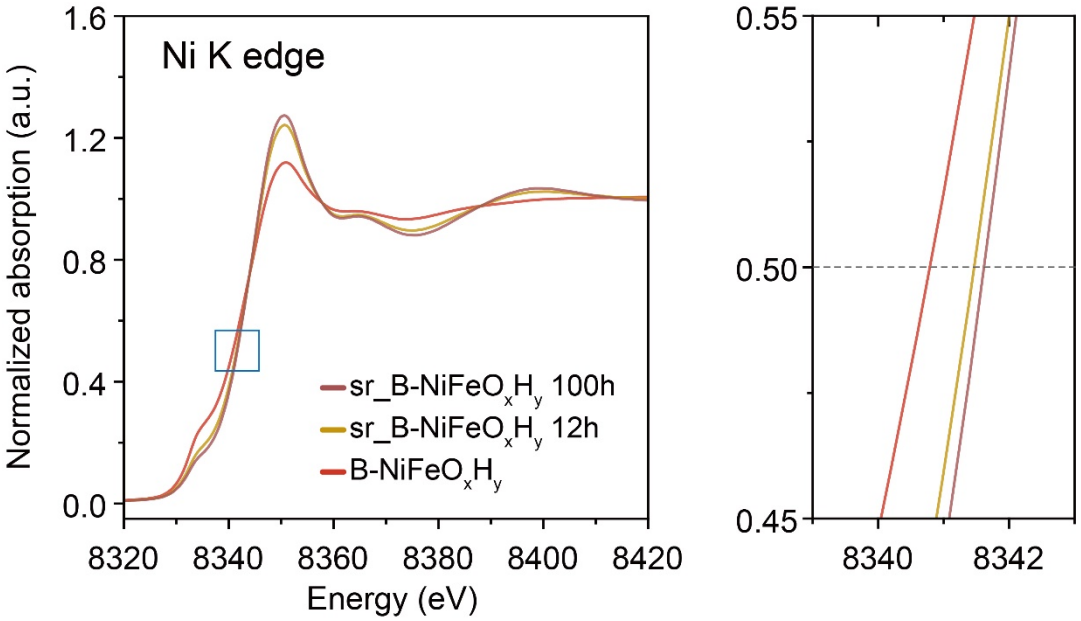

Fig. S23. The normalized Ni K-edge XAS analyses of B-NiFeO$_x$H$_y$ before and after 12 h and 100 h stability test.

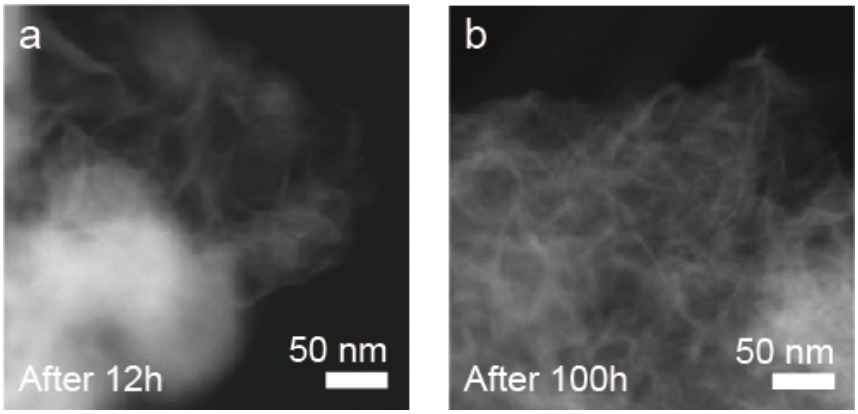

Fig. S24. Cs-corrected STEM images of sr_B-NiFeO_xH_y after long-term OER stability test: (a) After 12h and (b) After 100h.

Table S1. ICP-MS analysis of the as-prepared pristine B-$NiFeO_xH_y$ and $NiFeO_xH_y$.

Samples	Atomic ratio		
	Ni	**Fe**	**B**
B-$NiFeO_xH_y$	1	0.26	0.60
$NiFeO_xH_y$	1	0.25	0

Table S2. Comparison of OER performance of sr_B-$NiFeO_xH_y$ with other recently reported electrocatalysts in 1.0 M KOH.

Catalyst	Overpotential j_{10} (mV)	Tafel slope (mV dec^{-1})	Stability	Ref.
sr_B-$NiFeO_xH_y$	250	43	200 mA cm^{-2}@100h 200 mA cm^{-2}@79h at 55 °C in 30 wt% KOH	***This work***
$Ni^{vac}Fe^{vac}$-LDH	230	52	100 mA cm^{-2}@100h	S1
^{SA}Ru/NiFe LDH	251	98.1	10 mA cm^{-2}@8h	S2
NiFe-ANR	228	37	10 mA cm^{-2}@10h	S3
CoNiFe-LDH	257	31.4	10 mA cm^{-2}@60h	S4
NiFeCe-LDH	232	31.69	20 mA cm^{-2}@70h	S5
v-NiFe LDH	210	34.8	50 mA cm^{-2}@8h	S6
3D-NiFe-LDH	280 (j_{30})	50	200 mA cm^{-2}@10h	S7
NiFeSn@NiFe(Oxy)Hydroxide	260	50	10 mA cm^{-2}@11h	S8
PM-NiFe LDH	230	47	1.46 V@20h	S9
multi-layered NiFe LDH	260	27	500 mA cm^{-2}@20h at 80 °C	S10
Er-NiFe-LDH@NF	192	51.1	10 mA cm^{-2}@24h	S11
Ni_2Fe@Co-NC/CC	201	32.04	100 mA cm^{-2}@40h	S12

All electrochemical tests were conducted in 1.0 M KOH.

Table S3. Values of fitted parameters determined by fitting the Nyquist plot in Figure 2d where the units for resistance (R) and capacitance (constant phase element, Q) are Ω and $F \times s^{(1-a)}$ respectively.

Parameters	$\mathbf{R_s}$	$\mathbf{Q_1}$	$\mathbf{a_1}$	$\mathbf{R_1}$	$\mathbf{Q_2}$	$\mathbf{a_2}$	$\mathbf{R_{ct}}$
sr_B-$NiFeO_xH_y$	7.24	1.40×10^{-4}	0.61	2.48	1.87×10^{-2}	0.51	29.7
sr_$NiFeO_xH_y$	6.76	65.30	0.86	42.5	4.66×10^{-3}	0.42	168.5

Table S4. The inductively coupled plasma-mass spectrometry (ICP-MS) results and initially added ratio of Ni, Fe, and B during synthesis for each as-prepared sample. The amounts of $NaBH_4$ vary from 0.125, 0.25, 0.5, and 2 times compared to that of the B-$NiFeO_xH_y$ sample.

Samples	Resulting atomic ratio			Added ratio during synthesis		
	Ni	Fe	B	Ni	Fe	B
$B_{0.125}$-$NiFeO_xH_y$	1	1.18	0.054	1	0.25	0.312
$B_{0.25}$-$NiFeO_xH_y$	1	0.50	0.34	1	0.25	0.625
$B_{0.5}$-$NiFeO_xH_y$	1	0.28	0.65	1	0.25	1.25
B-$NiFeO_xH_y$	1	0.26	0.60	1	0.25	2.5
B_2-$NiFeO_xH_y$	1	0.26	0.60	1	0.25	5

Table S5. The atomic ratio of Ni: B ratio measured by XPS for each sample condition. " sr_B-$NiFeO_xH_y$ after 12 h" and "sr_B-$NiFeO_xH_y$ after 100 h" were taken after 12 h and 100 h of operation at 200 mA cm^{-2}, respectively.

Samples	Atomic ratio of Ni: B
As-prepared B-$NiFeO_xH_y$	0.52
sr_B-$NiFeO_xH_y$ after 12 h	0.40
sr_B-$NiFeO_xH_y$ after 100 h	0.42

Table S6. ICP-MS analysis of sr_B-NiFeO$_x$H$_y$ after 100 h of operation at 200 mA cm^{-2}.

Sample	Atomic ratio		
	Ni	**Fe**	**B**
sr_B-NiFeO$_x$H$_y$ after 100 h	1	0.28	0.34

Table S7. ICP-MS analysis of the bare carbon paper utilized within this work.

Sample	Element weight per carbon paper [mg/kg]		
	Ni	**Fe**	**B**
Bare carbon paper	0.47	3.52	0

References

[S1] L. Peng, N. Yang, Y. Yang, Q. Wang, X. Xie, D. Sun-Waterhouse, L. Shang, T. Zhang, G. I. Waterhouse, *Angew. Chem. Int. Ed.* **2021**, 60, 24612.

[S2] Y. Yang, Q.-N. Yang, Y.-B. Yang, P.-F. Guo, W.-X. Feng, Y. Jia, K. Wang, W.-T. Wang, Z.-H. He, Z.-T. Liu, *ACS Catal.* **2023**, 13, 2771.

[S3] X. Li, H. Zhang, Q. Hu, W. Zhou, J. Shao, X. Jiang, C. Feng, H. Yang, C. He, *Angew. Chem. Int. Ed.* **2023**, 62, e202300478.

[S4] J. Wu, T. Yang, R. Fu, M. Zhou, L. Xia, Z. Wang, Y. Zhao, *Adv. Funct. Mater.* **2023**, 2300808.

[S5] Y. Liao, R. He, W. Pan, Y. Li, Y. Wang, J. Li, Y. Li, *Chem. Eng. J.* **2023**, 464, 142669.

[S6] Y. Wang, S. Tao, H. Lin, G. Wang, K. Zhao, R. Cai, K. Tao, C. Zhang, M. Sun, J. Hu, *Nano Energy* **2021**, 81, 105606.

[S7] Z. Lu, W. Xu, W. Zhu, Q. Yang, X. Lei, J. Liu, Y. Li, X. Sun, X. Duan, *Chem. Commun.* **2014**, 50, 6479.

[S8] M. Chen, S. Lu, X. Z. Fu, J. L. Luo, *Adv. Sci.* **2020**, 7, 1903777.

[S9] X. Zhang, Y. Zhao, Y. Zhao, R. Shi, G. I. Waterhouse, T. Zhang, *Adv. Energy Mater.* **2019**, 9, 1900881.

[S10] R. Chen, S. F. Hung, D. Zhou, J. Gao, C. Yang, H. Tao, H. B. Yang, L. Zhang, L. Zhang, Q. Xiong, *Adv. Mater.* **2019**, 31, 1903909.

[S11] Y. Zhu, X. Wang, X. Zhu, Z. Wu, D. Zhao, F. Wang, D. Sun, Y. Tang, H. Li, G. Fu, *Small* **2023**, 19, 2206531.

[S12] T. You, K. Deng, P. Liu, X. Lv, W. Tian, H. Li, J. Ji, *Chem. Eng. J.* **2023**, 144348.